THE JOURNAL OF BIOLOGICAL CHEMISTRY
Vol. 272, No. 7, Issue of February 14, pp. 4391–4397, 1997

Printed in U.S.A.

Role of the Small GTPase RAB7 in the Late Endocytic Pathway*

(Received for publication, August 22, 1996, and in revised form, October 23, 1996)

Rosalba Vitelli‡, Mariarosaria Santillo§, Daniela Lattero, Mario Chiariello, Maurizio Bifulco¶, Carmelo B. Bruni‖, and Cecilia Bucci

From the Dipartimento di Biologia e Patologia Cellulare e Molecolare "L. Califano" and Centro di Endocrinologia ed Oncologia Sperimentale del Consiglio Nazionale delle Ricerche and §Dipartimento di Neuroscienze e della Comunicazone Interumana, Università di Napoli "Federico II," Via S. Pansini 5, 80131, Napoli, Italy and ¶Dipartimento di Medicina Sperimentale e Clinica, Università di Reggio Calabria, 88100 Catanzaro, Italy

Rab7 is a small GTPase localized to the late endosomal compartment. Its function was investigated by overexpressing dominant negative or constitutively active mutants in BHK-21 cells. The effects of such overexpression on the internalization and/or degradation of different endocytic markers and on the morphology of the late endosomal compartment were analyzed. We observed a marked inhibition of the degradation of ^{125}I-low density lipoproteins in cells transfected with the Rab7 dominant negative mutants while the rate of internalization was not affected. Moreover in these cells there was an accumulation of many small vesicles scattered throughout the cytoplasm. In contrast, overexpression of the activating mutants led to the appearance of atypically large endocytic structures and caused a dramatic change in the distribution of the cation-independent mannose 6-phosphate receptor. Our data indicate that the Rab7 protein in mammalian cells is present on a late endosomal compartment much larger than the compartment labeled by the cation-independent mannose 6-phosphate receptor. Rab7 also appears to play a fundamental role in controlling late endocytic membrane traffic.

Rab proteins are small GTPases localized at the cytoplasmic face of specific subcellular compartments in the endocytic and exocytic pathways. Several studies, using *in vitro* or *in vivo* assays, demonstrated a key role for these proteins in the regulation of intracellular vesicles trafficking (1, 2). Although the specific function of Rab proteins is not yet understood, the currently accepted model postulates that Rab proteins are required to assemble or proofread the general docking/fusion machinery (3).

The Rab7 protein has been previously localized to the late endosomal compartment in normal rat kidney (NRK) cells (4). Work from two different laboratories has demonstrated that Ypt7, the yeast Rab7 counterpart, is involved in transport to vacuoles and that expression of dominant negative mutants results in fragmentation of the vacuolar compartment (5, 6). Moreover it has been demonstrated that Ypt7 is required for vacuole fusion on both membrane partners (7). Recently the function of Rab7 has been investigated in mammalian cells (8, 9). However, the precise role of Rab7 in controlling endocytosis still remains under debate. Using stable cell lines overexpressing the wild type (wt)[1] or a GTPase-defective mutant protein (Rab7Q67L) and combining morphological and biochemical analyses, Chavrier and colleagues (9) showed that the mutant protein is in part associated with lysosomal membranes. The authors conclude that Rab7 cycles to lysosomes and suggest that it plays a role in a vesicular traffic step involving lysosomes (9). On the other hand Wandinger-Ness and co-workers (8), transiently expressing the Rab7 wt and two dominant negative mutants, demonstrated a role of the Rab7 protein in regulating early to late endosomes transport. The expression of the two mutant proteins (Rab7T22N and Rab7N125I) resulted in accumulation of the vesicular stomatitis virus G glycoprotein in the early endosomes and in a reduced cleavage of SV5 HN, a paramixovirus envelope protein (8). It has already been shown that a Rab protein can be present on more than a single cellular compartment and can control more than one transport step (10). However, in order to be able to regulate transport from early endosomes to lysosomes the Rab7 protein should be present in all these compartments.

In this study we have performed a detailed analysis of the Rab7 localization and function by transiently overexpressing several mutants in the BHK-21 cell line. We then investigated the changes induced by these proteins on the morphology of the late endosomal compartment and on the uptake and/or degradation of different endocytic markers, two of which (transferrin and LDL) are physiological ligands. Our results indicate that the Rab7 protein plays an important role in the organization of the late endosomal compartment and that its localization is not restricted to the cation-independent mannose 6-phosphate receptor (CI-MPR) positive compartment.

EXPERIMENTAL PROCEDURES

Plasmid Construction—Plasmids *Rab5, Rab5N133I*, and the human transferrin receptor have been previously described (11, 12). *Rab7* mutants were constructed by polymerase chain reaction-mediated mutagenesis (13). The oligonucleotides used in the first amplification for *Rab7T22N, Rab7I41M, Rab7Q67L, Rab7N125I,* and *Rab7ΔC* were, respectively: 5′-CTGGAGTTGGTAAGAATTCACTCATGAACCAG-3′, 5′-CAGAAAGTCTGCTCCCATTGTAGCTTTGTA-3′, 5′-GGAACCGTTCCAGGCCTGCTGTGTC-3′, 5′-CTGTTTTCGAGGTCAATCTTGATTCCCAACACAACGAAAGGGA-3′, and 5′-TTAAGCTTTCAGCTTTCCGCTGAGGTCTTG-3′. SP6 or T7 outer primers were used in all the amplifications. cDNAs encoding Rab5 and Rab7 wt and mutant proteins were cloned under the control of the T7 promoter in the pGEM1 or pGEM1-*myc* vectors (14) bearing a c-*myc* epitope (15). The constructs were completely sequenced to exclude the presence of *Taq* polymerase mistakes.

* This work was supported in part by a grant from Associazione Italiana per la Ricerca sul Cancro (to M. B.), Grant ERBFMRX-CT96-0020 from the European Economic Community (to C. B.), and a grant from the Comitato Nazionale per le Biotecnologie e la Biologia Molecolare (to C. B. B.). The costs of publication of this article were defrayed in part by the payment of page charges. This article must therefore be hereby marked "*advertisement*" in accordance with 18 U.S.C. Section 1734 solely to indicate this fact.

‡ Supported by a fellowship from the Associazione Italiana per la Ricerca sul Cancro.

‖ To whom correspondence should be addressed. Tel.: 0039-81-7462047; Fax: 0039-81-7703285.

[1] The abbreviations used are: wt, wild type; CI-MPR, cation-independent mannose 6-phosphate receptor; LDL, low density lipoproteins; LDS, lipoprotein-deficient serum; vT7, recombinant vaccinia T7 virus; PBS, phosphate-buffered saline.

Cell Culture and Transient Transfection—All tissue culture reagents were from Life Technologies, Inc. BHK-21 cells were grown in Glasgow minimal essential medium supplemented with 5% fetal calf serum, 10% tryptose phosphate broth, 2 mM glutamine, 100 units/ml penicillin, and 10 μg/ml streptomycin and grown in a 5% CO_2 incubator at 37 °C. BHK-21 cells were infected with the vT7 recombinant vaccinia virus and transfected as described (11). The transfection reagent was either DOTAP obtained by Boehringer Mannheim or made by sonicating dioleoyl-L-α-phosphatidylethanolamine and dimethyldioctadecyl ammonium bromide as described (16). Cells were transfected for 4–6 h and then processed for immunofluorescence or biochemical assays.

Antibodies and Confocal Immunofluorescence Microscopy—The 9E10 anti-myc monoclonal and the CI-MPR polyclonal antibodies were kind gifts from Dr. S. Fuller and Dr. B. Hofflack, respectively. The anti-Rab7 antibody was prepared as described (4). Anti-LY antibodies were bought from Molecular Probes. Cells grown on 11-mm round glass coverslips were permeabilized and fixed as described previously (11). The secondary antibodies fluorescein isothiocyanate- or tetramethylrhodamine isothiocyanate-conjugated anti-mouse or anti-rabbit were from Sigma or Amersham. Cells were viewed with the EMBL confocal microscope.

Western Blot and GTP Overlay—Cells were lysed in standard SDS sample buffer and extracts were electrophoresed on 12% SDS-polyacrylamide gels. For immunoblotting, separated proteins were transferred to nitrocellulose membrane. The filter was then blocked in 5% milk in PBS for 40 min at room temperature. Then primary mouse monoclonal 9E10 anti-myc antibody was added at the appropriate dilution and incubated for 2 h at room temperature. The filters were washed, incubated with a secondary anti-mouse horseradish peroxidase-conjugated antibody for 1 h at room temperature, and the bands were visualized using the enhanced chemiluminescence system (ECL, Amersham). For GTP overlay, after electrophoresis the gel was treated, transferred to nitrocellulose filter, and incubated with [α-^{32}P]GTP as described (11).

Estimation of Transferrin Binding, Endocytosis, and Recycling—Human transferrin (Sigma) was labeled to a specific activity of 10^7 cpm/mg using IODO-GEN (17). BHK-21 cells were transfected with the human transferrin receptor plasmid alone or together with the different plasmids encoding Rab7 wt and mutant proteins and treated as described (18, 19). The amount of transferrin endocytosed, recycled, and membrane bound was measured by γ-radiation counting.

Estimation of Horseradish Peroxidase Internalization—BHK-21 cells were transfected for 4 h with the plasmids encoding wild-type or mutant Rab7 proteins and then allowed to internalize horseradish peroxidase (5 mg/ml) in serum-free Glasgow minimal essential medium for times ranging from 1 to 60 min. Cells were then transferred on ice, washed extensively with PBS, 0.1% bovine serum albumin, and lysed in 10 mM Hepes (pH 7.4), 0.2% Triton X-100. The horseradish peroxidase content in the postnuclear supernatant was estimated using *o*-dianisidine (20). The total amount of protein was determined by colorimetric methods (21).

Internalization of Lucifer Yellow—Lucifer Yellow was diluted in Hank's balanced salt solution at a concentration of 5–10 mg/ml. Cells grown on 11-mm round glass coverslip were allowed to internalize Lucifer Yellow for 5–10 min at 37 °C. The cells were then washed extensively with Hanks' balanced salt solution and reincubated at 37 °C for various times in serum-deficient medium. After two washes with Hanks' balanced salt solution and one wash with PBS the cells were permeabilized, fixed, and processed for immunofluorescence.

Preparation of LDL and Labeling with ^{125}I—Human low density lipoprotein (LDL) ($1.019 < d < 1.063$ g/ml) was obtained by preparative ultracentrifugation (22) from serum of normolipidemic subjects to which 0.1% sodium azide, 1 mM EDTA disodium salt, and 0.17 TIU/ml of aprotinin were added, in order to prevent degradation of apoprotein. The h-LDL was then concentrated and further purified by double ultracentrifugation at density 1.063 g/ml. Lipoprotein-deficient serum (LDS) was prepared from the same serum samples used for LDL preparation by ultracentrifugation at density of 1.210 g/ml. h-LDL and LDS were then extensively dialyzed for 24 h at 4 °C against 0.15 M NaCl, 0.24 mM disodium EDTA (pH 7.4). The protein content of LDL, determined as described (23), ranged between 8 and 10 mg/ml. LDL was labeled with ^{125}I as described (24). The specific activity of ^{125}I-LDL ranged between 200 and 400 cpm/ng of protein; more than 98% ^{125}I radioactivity was precipitable by trichloroacetic acid and less than 3% was extractable in chloroform-methanol. Radioiodinated LDL was always used within 2 weeks from preparation.

Estimation of ^{125}I-LDL Internalization, Recycling, and Degradation—Cells were incubated for 24 h in medium complemented with human LDS before transfection. Transfected cells were allowed to internalize ^{125}I-LDL that was added to the medium at a concentration of 20 μg/ml for 5 h and the amount of ^{125}I-LDL surface bound, internalized, and degraded was estimated as described (25). Briefly, to determine the amount of ^{125}I-LDL degraded, the medium was collected, treated with trichloroacetic acid, extracted with chloroform and hydrogen peroxide to remove free iodine, and an aliquot of the aqueous phase was counted. This acid-soluble material is represented mainly by [^{125}I]iodotyrosine, the product of LDL degradation. To determine ^{125}I-LDL binding and internalization, after incubation with ^{125}I-LDL, cells were washed 6 times with PBS, 0.1% bovine serum albumin, once with PBS, and then treated with 3 mg/ml Pronase in serum-free medium containing 10 mM HEPES (pH 7.3) for 1 h at 0 °C. The cells were recovered by centrifugation at 3000 rpm for 3 min. The radioactivity present in the Pronase-medium (^{125}I-LDL surface bound), cell-associated (^{125}I-LDL internalized), and the acid-soluble material from the incubation medium (^{125}I-LDL degraded) was detected with a γ-counter.

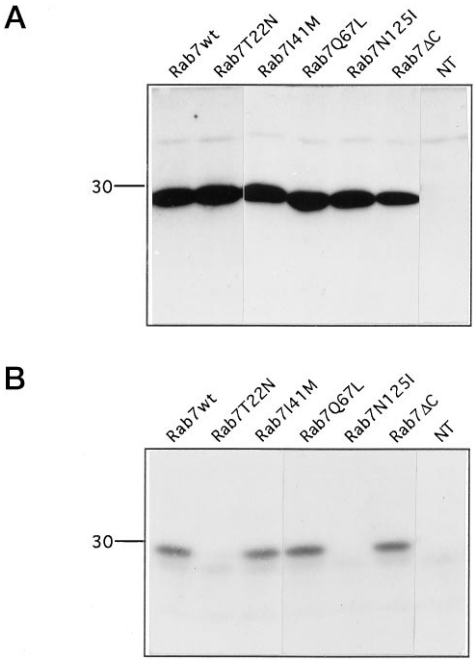

FIG. 1. **Western blot and GTP overlay on BHK-21 cells expressing myc-tagged Rab7 wt and mutant proteins.** *A*, Western blot analysis on lysates of BHK-21 cells infected with vT7 and transfected with pGEM1 encoding Rab7, Rab7T22N, Rab7I41M, Rab7Q67L, Rab7N125I, Rab7ΔC, or nontransfected (*NT*). The analysis was performed using monoclonal anti-myc antibodies as detailed under "Experimental Procedures." *B*, GTP overlay on the same lysates. [^{32}P]GTP binding was performed as described under "Experimental Procedures."

RESULTS

Construction and Expression of Rab7 Mutants in BHK-21 Cells—Using polymerase chain reaction-mediated mutagenesis (13) we introduced point mutations in the GTP binding or hydrolysis domain of the *Rab7* cDNA to obtain dominant negative or constitutively active mutants. Similarly to homologous mutations in *ras*, the mutant Rab7T22N should have a reduced affinity for GTP while the Rab7N125I should have a reduced guanine nucleotide binding. Analogous Rab5 mutant proteins (Rab5S34N and Rab5N133I) behaved as dominant negative mutants in both *in vitro* and *in vivo* assays (11, 19, 26, 27). On the other hand, the Rab7I41M and Rab7Q67L mutants are predicted to have an impaired intrinsic (Rab7Q67L) or GAP-mediated (Rab7I41M) GTP hydrolysis and should preferentially be in the GTP-bound form. The Rab7ΔC mutant has the last three amino acids deleted. This mutant lacks the cysteines required for membrane association and remains cytosolic (data not shown).

We expressed all the constructs in BHK-21 cells using the vaccinia recombinant VT7 infection/transfection system (28). Fig. 1 shows a Western blot (*A*) and a GTP-binding blot (*B*) of

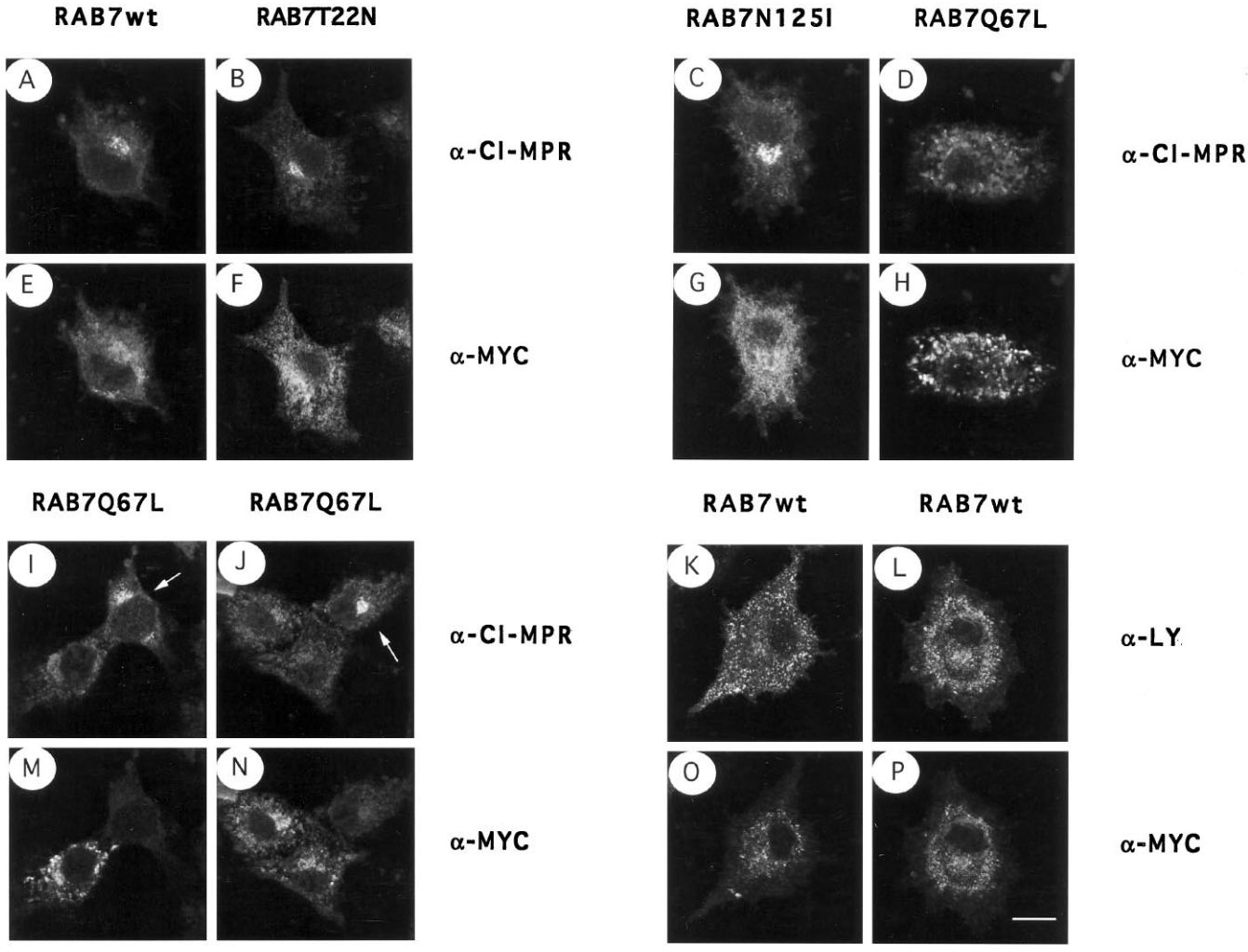

FIG. 2. **Immunofluorescence analysis of cells overexpressing the Rab7 wt or mutant proteins.** Cells were transfected for 4 h with Rab7 wt (*A*, *E*, *K*, *L*, *O*, and *P*), RabT22N (*B* and *F*), Rab7Q67L (*D*, *H-J*, *M*, and *N*), or Rab7N^{125}I (*C* and *G*). Before fixation some transfected cells were incubated for 5 min (*K* and *O*) or 30 min (*L* and *P*) in the presence of 10 mg/ml Lucifer Yellow (*LY*). Analysis was performed using monoclonal anti-myc antibody to detect Rab proteins (*E-H*; *M-P*) or polyclonal anti-CI-MPR (*A-D*; *I-J*) or polyclonal anti-LY (*K-L*). The constructs used for the transfection are indicated on *top* and the primary antibodies used in the immunofluorescence on the *right side* of the panels.

BHK-21 cells infected with the vT7 virus and transfected with the *wt* or mutant Rab7 *myc*-tagged plasmids. As a control we used cells that were infected with the vT7 virus but nontransfected. Western blot analysis was performed with a monoclonal anti-myc antibody. The *myc*-tagged Rab7 wt and mutant proteins were expressed at comparable levels (Fig. 1*A*) and more than 15-fold over the endogenous levels (data not shown). This high expression was reached because of the presence of a perfect Kozak consensus sequence in front of the *myc* epitope (14). As expected, the Rab7 wt and the Rab7I41M, Rab7Q67L, and Rab7ΔC mutant proteins bind efficiently GTP whereas the Rab7T22N or Rab7N125I proteins do not bind the nucleotide (Fig. 1*B*).

Immunofluorescence Analysis of Cells Expressing Rab7 wt or Mutant Proteins—The Rab7 protein was previously localized to the late endosomes in BHK-21, Madin-Darby canine kidney, and NRK cells (4). We analyzed by double immunofluorescence the effect of the overexpression of the Rab7 wt and mutant proteins on the late endosomal compartment in BHK-21 cells. We used the monoclonal anti-myc antibody to detect the myc-tagged overexpressed proteins and a polyclonal anti-CI-MPR antibody to identify the late endosomal compartment. The CI-MPR is localized to early endosomes, late endosomes, and *trans*-Golgi network but the bulk of the protein is in the late endosomal compartment (29). Overexpression of the myc-tagged Rab7 wt protein results in the staining of a vesicular compartment mainly confined to the perinuclear area (Fig. 2*E*), similar to the localization of the endogenous protein (4). Surprisingly, there was only partial co-localization between the myc-tagged Rab7 wt protein and the CI-MPR in BHK-21 cells (Fig. 2, *A* and *E*). The two proteins were in the same perinuclear area but the wt Rab7 staining was more widely distributed in the cell compared to the CI-MPR staining. This would suggest that the CI-MPR is present only in restricted regions of the late endosomal compartment or that Rab7 is not confined to late endosomes. Expression of the two dominant negative mutants, Rab7T22N (Fig. 2*F*) or Rab7N125I (Fig. 2*G*), in BHK-21 cells resulted in the labeling of small vesicles scattered throughout the cytoplasm and also present under the plasma membrane. In contrast, the expression of the two activating mutants, Rab7I41M (data not shown) or Rab7Q67L (Fig. 2, *H*, *M*, and *N*), led to the formation of larger vesicles again not restricted to the perinuclear area. The distribution of the CI-MPR also changed dramatically upon overexpression of Rab7Q67L. Normally, the CI-MPR staining was mainly restricted to perinuclear structures such as in cells transfected with Rab7 wt, Rab7T22N, and Rab7N125I (Fig. 2, *A-C*). When the Rab7Q67L was expressed the CI-MPR staining was no longer confined to these perinuclear structures (Fig. 2*D*). Other cells transfected with Rab7Q67L are shown in Fig. 2, *I*, *J*, *M*,

and *N*. Arrows indicate nontransfected cells in which the distribution of the CI-MPR was unaffected. Expression of the Rab7ΔC mutant resulted in a cytosolic localization of this protein and had no effect on the distribution of the CI-MPR (data not shown).

The Rab7 Compartment Is Reached by Lucifer Yellow—Lucifer Yellow is a fluid phase endocytic marker that labels early endosomes in the first 5–10 min of internalization and, after longer incubation times, late endosomes and lysosomes. We investigated whether this marker was able to stain the Rab7 compartment. Cells transfected with the different constructs were first allowed to internalize Lucifer Yellow for 5 min to primarily label the early endosomal compartment. After extensive washing the cells were reincubated at 37 °C for various times to allow accumulation of the marker in late endosomes and lysosomes. 5 min of internalization were sufficient to detect the Lucifer Yellow marker in small vesicles scattered throughout the cell. No co-localization with the Rab7 wt protein, that was mainly restricted to the perinuclear area (Fig. 2, *K* and *O*) or with any other Rab7 mutant protein (data not shown), was observed. After 30 min of chase Lucifer Yellow was mainly present in the perinuclear region and found to co-localize with the Rab7 wt protein (Fig. 2, *L* and *P*). A similar co-localization was found when the different Rab7 mutant proteins were expressed (data not shown).

Transferrin and Horseradish Peroxidase Endocytosis Are Not Altered in BHK-21 Cells Overexpressing Rab7 wt and Mutant Proteins—To analyze the effect of the overexpression of the Rab7 mutant proteins on the first steps of endocytosis we measured the internalization of transferrin and horseradish peroxidase.

Transferrin binds iron at the cell surface, is clustered into coated pits, and is internalized by coated vesicles. It is then transported to the early endosomes where it looses the iron and is recycled back to the membrane together with its receptor. Overexpression of Rab5 doubles the rate of internalization of transferrin whereas expression of the dominant negative mutant Rab5N133I inhibits endocytosis of this marker, as described previously (11, 18, 19). As expected the initial rate of internalization of ^{125}I-transferrin was altered in cells expressing Rab5 or Rab5N133I but no significant change was detectable upon overexpression of Rab7 wt or any of the Rab7 mutants. After 5 min there was a 70% increase in the amount of internalized transferrin in cells overexpressing the wt Rab5 protein and a 30% decrease in cells expressing the Rab5N133I mutant protein (Fig. 3*A*). Overexpression of all the Rab7 constructs also did not affect the recycling of ^{125}I-transferrin to the plasma membrane (data not shown).

Horseradish peroxidase is currently used as a marker of fluid phase endocytosis. Overexpression of Rab5 and Rab5N133I mutant changes the amount of horseradish peroxidase internalized in the cells (11). Overexpression of Rab5 wt doubles the amount of horseradish peroxidase accumulated in the cells after 60 min of internalization, while the expression of the Rab5N133I mutant causes a 30% decrease (Fig. 3*B*). No significant changes were detected after overexpression of the Rab7 wt or mutant proteins at this (Fig. 3*B*) and at earlier or later time points (data not shown).

LDL Degradation Is Severely Affected by the Expression of Dominant Negative Rab7 Mutants—To study the effect of Rab7 on the endocytic pathway we examined the internalization and degradation of ^{125}I-LDL in BHK-21 cells overexpressing the Rab7 wt and mutant proteins. LDL binds a specific receptor on the surface of cultured fibroblast with high affinity. LDL is internalized and degraded, so that its cholesterol component is made available for cellular membrane synthesis while the receptor is recycled to the plasma membrane. Only a very small amount of LDL is recycled to the plasma membrane.

Before transfection, BHK-21 cells were incubated for 24 h in medium complemented with human LDS. After transfection the cells were allowed to internalize ^{125}I-LDL added to the medium at a concentration of 20 μg/ml for 5 h and the amount of ^{125}I-LDL surface bound, internalized, and degraded was estimated as described under "Experimental Procedures." Fig. 4 shows a typical experiment of ^{125}I-LDL internalization (Fig. 4*A*) and degradation (Fig. 4*B*). The accumulation of ^{125}I-LDL in BHK-21 cells showed a 50% increase in cells overexpressing Rab5 (Fig. 4*A*). This is consistent with the contention that the Rab5 protein is able to accelerate the kinetics of endocytosis (11). An increase of approximately 50% in the intracellular accumulation of ^{125}I-LDL was also observed in cells expressing Rab7T22N and Rab7N125I, compared to control cells (Fig. 4*A*). However, this effect was accompanied by a strong inhibition (more than 60%) of the degradation of LDL (Fig. 4*B*). Inhibition of ^{125}I-LDL degradation was also observed in cells transfected with the Rab5N133I mutant protein but in this case the amount of ^{125}I-LDL internalized was approximately 30% less than in control cells (Fig. 4*A*). This is consistent with previous findings that dominant negative mutants of Rab5 inhibit endocytosis (11, 18, 19).

No effect on ^{125}I-LDL intracellular accumulation or degradation was detected upon overexpression of the Rab7ΔC mutant compared to control cells. This is consistent with the hypothesis that this mutant is not post-translationally modified, is not able to attach to the membrane, and therefore is not functional.

To demonstrate that Rab7 did not interfere with the first steps of endocytosis we measured the initial internalization rate of ^{125}I-LDL in cells expressing the Rab7 and Rab5 wt and mutant proteins (data not shown). After transfection cells were allowed to bind ^{125}I-LDL for 2 h at 4 °C and the excess of unbound ligand was removed by washing. In all transfected cells the number of surface ^{125}I-LDL-binding sites was similar and 90% of ^{125}I-LDL was specifically bound. To measure the rate of uptake the cells were then shifted at 37 °C for different periods of time ranging from 30 s to 60 min and the fraction of internalized ^{125}I-LDL was determined. After 5 min control cells had internalized 70% of prebound ^{125}I-LDL while cells expressing the dominant negative mutants of Rab5 had internalized only 40%. Conversely, the internalization rate of ^{125}I-LDL was accelerated in cells expressing the Rab5 wt protein since in these cells about 70% of the prebound ^{125}I-LDL was internalized within 2.5 min. These data are consistent with previous studies showing that Rab5 regulates the kinetics of receptor-mediated endocytosis (11, 19). No effect was detected on the initial internalization rate upon overexpression of Rab7 wt or any mutant protein (data not shown).

These data demonstrate that Rab5 and Rab7 have distinct roles in regulating the endocytic pathway. While Rab5 controls the early steps and is able to modify the kinetics of endocytosis, Rab7 does not influence the initial steps of the pathway but has a fundamental role in regulating transport to late endocytic compartments.

DISCUSSION

In this paper we have studied the role of Rab7 in the endocytic pathway. We transiently expressed in BHK-21 cells several mutants of the protein with impaired ability to bind or hydrolyze GTP and we monitored their effect on the morphology of the late endosomal compartment and on the internalization and/or degradation of different endocytic markers.

We demonstrated that Rab7 plays an important role in late

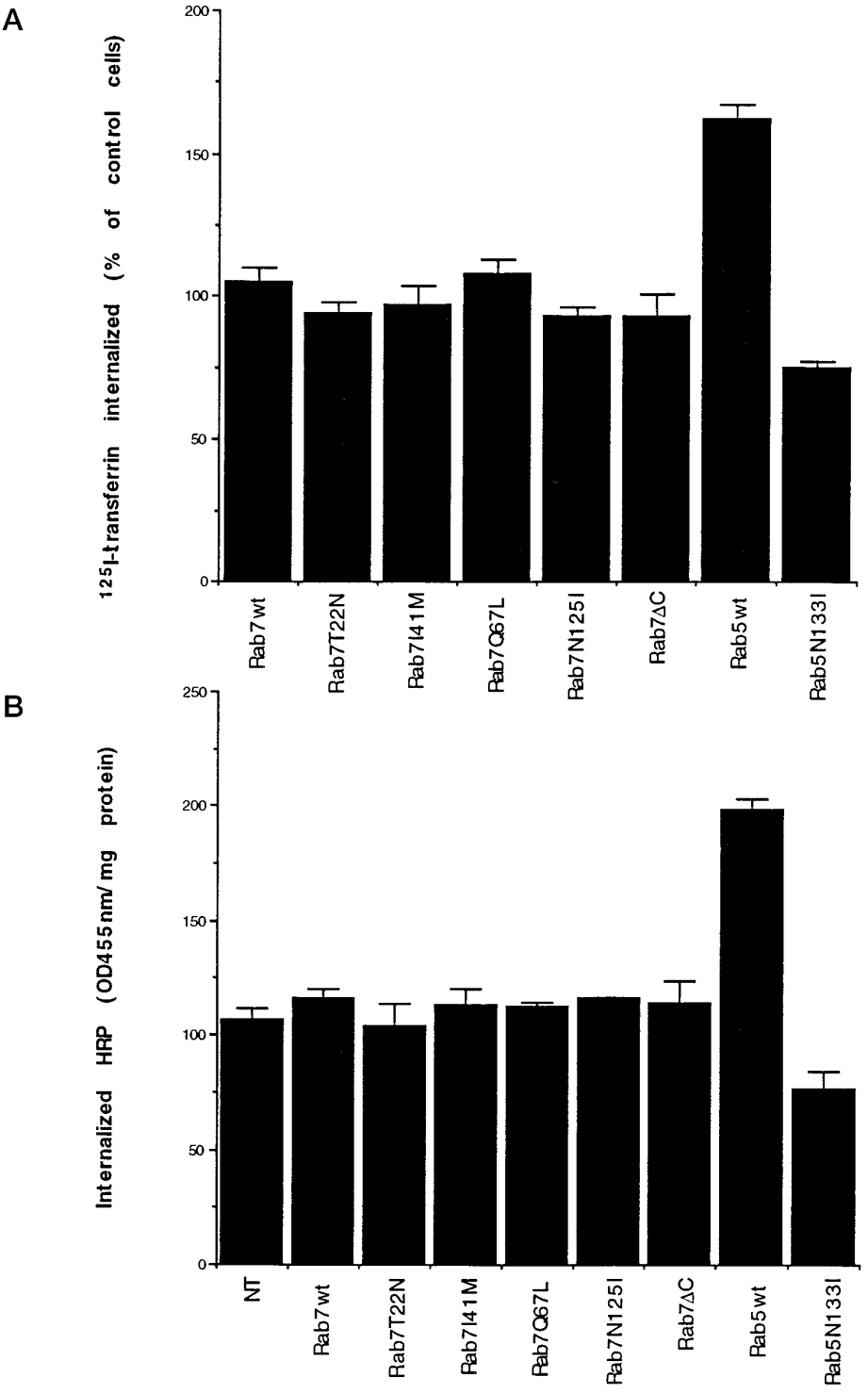

FIG. 3. **Expression of Rab7 wt and mutant proteins does not affect transferrin or horseradish peroxidase (*HRP*) endocytosis.** *A*, HeLa cells were infected with vT7 and transfected for 4 h with the human transferrin receptor alone (control cells) or together with the indicated plasmids. Cells were incubated at 4 °C for 1 h with ^{125}I-transferrin, washed, and then reincubated at 37 °C for 5 min to allow internalization. The amount of internalized transferrin is plotted as percentage of control cells. *B*, BHK-21 cells were infected with vT7 and either not transfected (*NT*) or transfected with the indicated plasmids. After 4 h of transfection cells were allowed to internalize horseradish peroxidase present in the medium at a concentration of 2 mg/ml for 30 min. Cells were then washed, lysed, and the amount of internalized horseradish peroxidase was measured. The data represent the average of three independent experiments with *error bars*.

steps of endocytosis since the expression of the two dominant negative mutant proteins causes a marked inhibition of the degradation of ^{125}I-LDL while the initial internalization rate remains unchanged. Moreover, no effect of the expression of any Rab7 mutant protein was detected in the internalization and/or recycling of transferrin or horseradish peroxidase. These findings show that Rab7 does not function in the early endocytic pathway and does not influence the kinetics of internalization. The early steps of endocytosis are instead regulated by the Rab5 proteins (18). Rab7 therefore functions in a later step compared to Rab5 and influences the late endosome organization. Consistent with this conclusion, expression of different mutants impaired in their ability to bind or hydrolyze GTP causes big changes in the morphology of the compartment as judged by the immunofluorescence distribution of CI-MPR and the Rab7 mutant proteins.

The Rab7 protein has been previously localized to late endosomes in NRK cells by co-localization with the CI-MPR by electron microscopy studies (4). However, surprisingly, the protein seems to be present mainly in a CI-MPR negative compartment in BHK-21 cells. This compartment is labeled in 30 min by Lucifer Yellow, a fluid phase marker of the endocytic pathway, suggesting that the CI-MPR labels only restricted areas of the late endosomal compartment (Fig. 2). Remarkably, we also noticed a drastic change in the distribution of the CI-MPR upon expression of the Rab7Q67L constitutively active

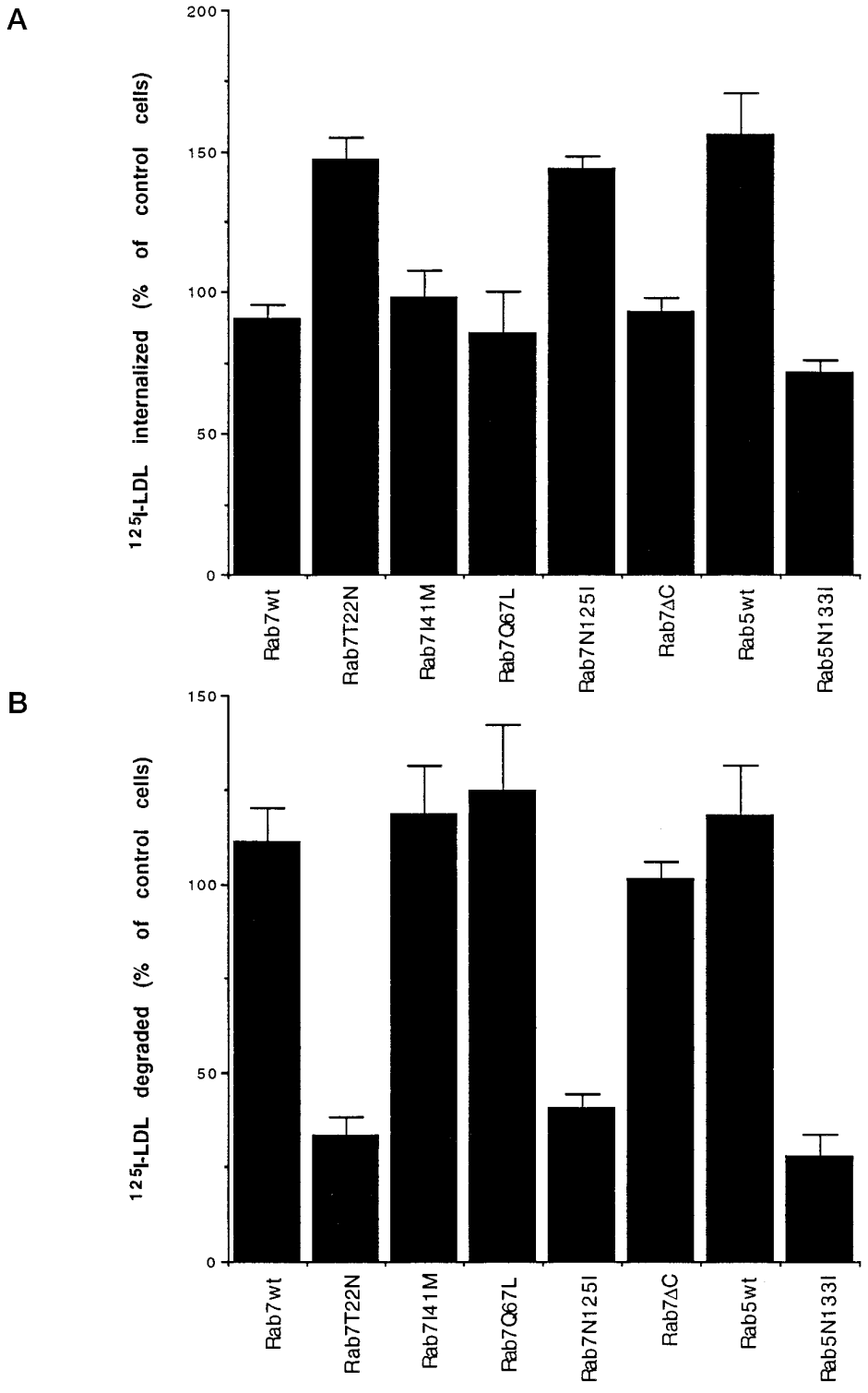

FIG. 4. **Effects of expression of Rab7 wt and the various mutant on ^{125}I-LDL internalization and degradation.** Cells were grown for 24 h in LDS, infected with the vT7 recombinant vaccinia virus, and transfected with the different constructs as indicated. After 4 h of transfection cells were washed extensively and incubated 5 h at 37 °C in the presence of 20 μg/ml ^{125}I-LDL. The amount of ^{125}I-LDL internalized (*A*) or degraded (*B*) is plotted as percentage of control cells. The data represent the average of five independent experiments with *error bars*.

mutant. These data disagree with a previous report in which the distribution of the CI-MPR in a stable cell line expressing the Rab7Q67L did not show any detectable change (9). The organization of the endosomal compartment seems to be quite different between BHK-21 cells, used in this study, and the inducible HeLa cell lines used by Chavrier and colleagues (9). However, we have transiently expressed the Rab7Q67L mutant also in HeLa cells and could detect a similar effect even if less pronounced (data not shown). One possible explanation for this discrepancy is that in our experiments the use of the vT7 infection/transfection expression system causes a higher level of expression of the mutant protein (more than 15-fold over the endogenous) in a very short time (4 h). In the stable cell lines used by Chavrier and colleagues (9) lower levels of expression (4–5-fold over the endogenous) were achieved after a very long time (3 days of induction). During this time cells may have

adapted to the presence of the Rab7Q67L protein and might have been able to overcome the redistribution of the CI-MPR.

The expression of the constitutively active Rab7Q67L protein causes the formation of large endocytic structures while expression of the two dominant negative mutants (Rab7T22N and Rab7N125I) gives a very fine and punctate staining. These effects resemble those produced by Rab5 on early endosomes. Expression of the Rab5Q79L activating mutant induces the formation of giant early endosomes while expression of the Rab5N133I mutant causes accumulation of small vesicles and tubules at the periphery of the cell (11, 19, 26, 27). Since the effect of Rab5 is due to its ability to control fusion at the level of early endosomes one could imagine the same to be true for Rab7 at the level of late endosomes. This hypothesis is confirmed by the fact that ^{125}I-LDL degradation is inhibited in cells expressing the Rab7T22N and Rab7N125I mutant proteins. In these cells a delayed delivery to the late endocytic compartment due to inhibition of fusion would prevent efficient degradation of ^{125}I-LDL and would allow its accumulation in the cells (Fig. 4).

Our data do not discriminate whether the Rab7 protein controls early to late endosomes or late endosomes to lysosomes transport or both. The development of *in vitro* assays to study these two different steps will be required to solve this issue. However, our results indicate that the Rab7 protein plays a fundamental role in the endocytic pathway at the level of late endosomes, probably controlling fusion. This is demonstrated by the morphological changes of the compartment upon overexpression of the Rab7 wt and mutant proteins and by the strong effect on LDL degradation upon expression of the dominant negative mutants.

Further characterization of this late endosomal compartment by morphological and biochemical assays together with the identification of interacting components of Rab7 will be required to pinpoint the site of action of this protein and gain complete understanding of its role in the late endocytic pathway.

Acknowledgments—We thank Marino Zerial and Pietro Alifano for critical reading of the manuscript and Mario Berardone for photographic work. C. Bucci also thanks all the members of Marino Zerial laboratory for constant encouragement during the course of this study.

REFERENCES

1. Zerial, M., and Stenmark, H. (1993) *Curr. Opin. Cell Biol.* **5,** 613–620
2. Simons, K., and Zerial, M. (1993) *Neuron* **11,** 789–799
3. Rothman, J. E. (1994) *Nature* **372,** 55–63
4. Chavrier, P., Parton, R. G., Hauri, H. P., Simons, K., and Zerial, M. (1990) *Cell* **62,** 317–329
5. Wichmann, H., Hengst, L., and Gallwitz, D. (1992) *Cell* **71,** 1131–1142
6. Schimmoller, A., and Riezman, H. (1993) *J. Cell Sci.* **106,** 823–830
7. Haas, A., Scheglmann, D., Lazar, T., Gallwitz, D., and Wickner, W. (1995) *EMBO J.* **14,** 5258–5270
8. Feng, Y., Press, B., and Wandinger-Ness, A. (1995) *J. Cell Biol.* **131,** 1435–1452
9. Méresse, S., Gorvel, J.-P., and Chavrier, P. (1995) *J. Cell Sci.* **108,** 3349–3358
10. Plutner, H., Cox, A. D., Pind, S., Khosravi-Far, R., Bourne, J. R., Schwaninger, R., Der, C. J., and Balch, W. E. (1991) *J. Cell Biol.* **115,** 31–43
11. Bucci, C., Parton, R. G., Mather, I. H., Stunnenberg, H., Simons, K., Hoflack, B., and Zerial, M. (1992) *Cell* **70,** 715–728
12. Gorvel, J.-P., Chavrier, P., Zerial, M., and Gruenberg, J. (1991) *Cell* **64,** 915–925
13. Landt, O., Grunert, H.-P., and Hahn, U. (1990) *Gene* (*Amst.*) **96,** 125–128
14. Olkkonen, V. M., Dupree, P., Killisch, I., Lütcke, A., Zerial, M., and Simons, K. (1993) *J. Cell Sci.* **106,** 1249–1261
15. Evan, G. I., Lewis, G. K., Ramsay, G., and Bishop, J. M. (1985) *Mol. Cell Biol.* **5,** 3610–3616
16. Rose, J. K., Buonocore, L., and Whitt, M. A. (1991) *BioTechniques* **10,** 520–525
17. Podbilewicz, B., and Mellman, I. (1990) *EMBO J.* **9,** 3477–3487
18. Bucci, C., Lütcke, A., Steele-Mortimer, O., Chiariello, M., Olkkonen, V. M., Dupree, P., Bruni, C. B., Simons, K., and Zerial, M. (1995) *FEBS Lett.* **366,** 65–71
19. Stenmark, H., Parton, R. G., Steele-Mortimer, O., Lütcke, A., Gruenberg, J., and Zerial, M. (1994) *EMBO J.* **13,** 1287–1296
20. Marsh, M., Schmid, S., Kern, H., Harms, E., Male, P., Mellman, I., and Helenius, A. (1987) *J. Cell Biol.* **104,** 875–886
21. Bradford, M. M. (1976) *Anal. Biochem.* **72,** 248–254
22. Havel, R. S., Eder, H. A., and Bragdon, S. H. (1955) *J. Clin. Invest* **34,** 1345–1353
23. Lowry, O. H., Rosebrough, N. J., Farr, A. L., and Randall, R. J. (1951) *J. Biol. Chem.* **193,** 265–275
24. Bilheimer, D. W., Eisenberg, S., and Levy, R. I. (1972) *Biochim. Biophys. Acta* **262,** 212–221
25. Brown, M. S., and Goldstein, J. L. (1975) *Cell* **6,** 307–316
26. Li, G., Barbieri, M. A., Colombo, M. I., and Stahl, P. D. (1994) *J. Biol. Chem.* **269,** 14631–14635
27. Li, G., and Stahl, P. D. (1993) *J. Biol. Chem.* **268,** 24475–24480
28. Fuerst, T. R., Niles, E. G., Studier, F. W., and Moss, B. (1986) *Proc. Natl. Acad. Sci. U. S. A.* **83,** 8122–8126
29. Griffiths, G., Hoflack, B., Simons, K., Mellman, I., and Kornfeld, S. (1988) *Cell* **52,** 329–341

Role of the Small GTPase RAB7 in the Late Endocytic Pathway

Rosalba Vitelli, Mariarosaria Santillo, Daniela Lattero, Mario Chiariello, Maurizio Bifulco, Carmelo B. Bruni and Cecilia Bucci

J. Biol. Chem. 1997, 272:4391-4397.
doi: 10.1074/jbc.272.7.4391
